Cationic Comb Polymer Superdispersants for Colloidal Silica Suspensions

Summer K. Rhodes,[†] Robert H. Lambeth,[‡,§] Jaime Gonzales,[||] Jeffrey S. Moore,[†,‡,§] and Jennifer A. Lewis*,[†]

[†]*Materials Science and Engineering Department, Frederick Seitz Materials Research Laboratory and* [‡]*Chemistry Department and* [§]*The Beckman Institute for Advanced Science and Technology, and* [||]*Department of Molecular and Cell Biology, University of Illinois, Urbana, Illinois 61801*

We investigate the ability of a cationic comb polymer composed of a poly(trimethylammonium iodide ethyl methacrylate) (PTMAM) backbone and uncharged poly(ethylene glycol) (PEG) teeth to stabilize aqueous silica suspensions of varying ionic strength and pH. Both PTMAM-*g*-PEG and its homopolymer backbone, PTMAM, are synthesized via reversible addition−fragmentation chain transfer followed by quaternization of the pendant amine groups with methyl iodide. Through a combination of polymer adsorption, zeta potential, and sedimentation measurements as well as confocal imaging of sediment structures, we find that PTMAM-*g*-PEG imparts stability over a broad range of solution conditions, where pure PTMAM fails.

Introduction

Cationic polyelectrolytes, such as poly(dimethylaminoethyl methacrylate) (PDMAM), are widely used as dispersants to impart electrosteric stability to colloidal silica suspensions.[1−4] PDMAM is a weak polyelectrolyte whose amine groups become increasingly protonated with decreasing pH.[2,5−7] However, when functionalized with quaternary ammonium groups, it becomes a strong polyelectrolyte that is fully ionized over a wide pH range.[3,8]

The difference in ionization behavior between the weak and quaternized derivatives of PDMAM[5−10] have a marked effect on their adsorption behavior on silica. Silica microspheres exhibit an isoelectric point near pH ~ 2−3 and, hence, become more negatively charged as the solution pH increases above this value. The adsorption of nonquaternized PDMAM species onto silica colloids first increases with pH and then decreases at even higher pH values as the chains become weakly ionized. By contrast, poly(trimethylammonium iodide ethyl methacrylate) (PTMAM), a quaternized derivative of PDMAM, exhibits enhanced adsorption onto silica colloids with increasing pH.

Pure polyelectrolytes are often only effective at providing colloidal stability within a narrow range of ionic strength and pH values.[11−14] For example, at high ionic strengths, counterions effectively screen the charged groups present along the polyelectrolyte backbone, simultaneously leading to the collapse of adsorbed chains on the colloid surfaces, and possibly even ion bridging in the presence of multivalent species.[15,16] Typically, particle flocculation ensues under such conditions, since the electrosteric barrier that provides stability is dramatically reduced.[12,13] In related work, Lewis and co-workers have shown that anionic comb copolymers composed of a poly(acrylic acid) (PAA) backbone with poly(ethylene oxide) (PEO) teeth are able to stabilize colloidal suspensions, including both cementitious[17] and barium titanate[18,19] systems, over a broad range of solution conditions, where pure PAA fails. Based on their observations, they proposed that the uncharged PEO teeth not only protect the underlying polyelectrolyte backbone from ion bridging interactions, the teeth also provide a robust steric barrier that resists flocculation. To our knowledge, cationic analogues of these comb polymers have yet to be explored as dispersants for colloidal suspensions, such as silica or titania, whose isoelectric points occur under acidic conditions.

Here, we investigate the ability of a cationic comb polymer composed of a PTMAM backbone and uncharged PEG teeth to stabilize aqueous silica suspensions of varying ionic strength and pH. We compare these observations to those obtained for pure PTMAM, which serves as a benchmark in this study. Through a combination of polymer adsorption, zeta potential, sedimentation measurements, and confocal imaging, we show that PTMAM-*g*-PEG serves as a "superdispersant" that provides stability over a broad range of solution conditions, in which PTMAM-coated silica microspheres experience rapid flocculation. These cationic

(1) Lewis, J. A. *J. Am. Ceram. Soc.* **2000**, *83*, 2341–2359.

(2) Hansupalak, N.; Santore, M. M. *Langmuir* **2003**, *19*, 7423–7426.

(3) Hoogeveen, N. G.; Stuart, M. A. C.; Fleer, G. J. *J. Colloid Interface Sci.* **1996**, *182*, 133–145.

(4) Meszaros, R.; Thompson, L.; Bos, M.; de Groot, P. *Langmuir* **2002**, *18*, 6164–6169.

(5) Hansupalak, N.; Santore, M. M. *Macromolecules* **2004**, *37*, 1621–1629.

(6) Shin, Y. W.; Roberts, J. E.; Santore, M. *J. Colloid Interface Sci.* **2001**, *244*, 190–199.

(7) Shin, Y. W.; Roberts, J. E.; Santore, M. M. *J. Colloid Interface Sci.* **2002**, *247*, 220–230.

(8) Jones, M., Jr. *Organic Chemistry*, 2nd ed.; W. W. Norton & Company: New York, 2000.

(9) Hoogeveen, N. G.; Stuart, M. A. C.; Fleer, G. J. *J. Colloid Interface Sci.* **1996**, *182*, 146–157.

(10) Shin, Y.; Roberts, J. E.; Santore, M. M. *Macromolecules* **2002**, *35*, 4090–4095.

(11) Dahlgren, M. A. G. *Langmuir* **1994**, *10*, 1580–1583.

(12) de la Cruz, M. O.; Belloni, L.; Delsanti, M.; Dalbiez, J. P.; Spalla, O.; Drifford, M. *J. Chem. Phys.* **1995**, *103*, 5781–5791.

(13) Solis, F. J.; de la Cruz, M. O. *J. Chem. Phys.* **2000**, *112*, 2030–2035.

(14) Vermohlen, K.; Lewandowski, H.; Narres, H. D.; Schwuger, M. *J. Colloids Surf., A* **2000**, *163*, 45–53.

(15) Atkin, R.; Craig, V. S. J.; Biggs, S. *Langmuir* **2000**, *16*, 9374–9380.

(16) Liufu, S. C.; Xiao, H. N.; Li, Y. P. *J. Colloid Interface Sci.* **2005**, *285*, 33–40.

(17) Kirby, G. H.; Lewis, J. A. *J. Am. Ceram. Soc.* **2004**, *87*, 1643–1652.

(18) Kirby, G. H.; Harris, D. J.; Li, Q.; Lewis, J. A. *J. Am. Ceram. Soc.* **2004**, *87*, 181–186.

(19) Yoshikawa, J.; Lewis, J. A.; Chun, B. W. *J. Am. Ceram. Soc.* **2009**, *92*, S42–S49.

comb polymer dispersants may find potential application in colloidal suspensions designed for photonic crystal assembly,[20−22] inks for direct writing,[23] drug delivery,[24−27] or other biomedical applications.[25,28,29] Furthermore, they provide a new pathway for producing biphasic colloidal mixtures,[30] in which comb polymer and pure polyelectrolyte-coated microspheres are combined under appropriate solution conditions.

Experimental Section

Polymer Synthesis. PTMAM-*g*-PEG and PTMAM dispersants are prepared by reversible addition−fragmentation chain transfer (RAFT) polymerization followed by quaternization with methyl iodide (MeI). PTMAM-*g*-PEG is produced from a feedstock consisting of a 7:1 molar ratio of DMAM monomer to methacrylate-functionalized PEG (number average molecular weight, $M_n = 2080$). The polymer chains are isolated by dialysis (M_n cutoff = 10 kDa) against water for 72 h, followed by freeze-drying. Their M_n is 30 000 and 66 000 g/mol for PTMAM and PTMAM-*g*-PEG, respectively, as determined by gel permeation chromatography (GPC). The amine groups present along the PTMAM backbone are converted to quaternary ammonium ions through methylation with MeI. Full synthetic details and characterization are provided in the Supporting Information.

Polymer Solution Characterization. The radius of hydration (R_h) of PTMAM-*g*-PEG and PTMAM is determined by capillary viscometry using a Ubbelohde viscometer (model 9722-M53, Cannon Inst. Co., State College, PA) placed in a constant temperature bath at 30 ± 0.1 °C. Flow-time measurements are carried out on dilute polymer solutions (∼0.01−0.02 g/mL, pH 6) of varying salt concentration (1 mM to 1 M sodium chloride, NaCl). The relative viscosities, η_{rel}, are measured at five different polymer concentrations, c, where η_{rel} is defined by the ratio of the flow time of a given polymer solution to that of the pure solvent. From these data, the intrinsic viscosity, $[\eta]$, is given by

$$[\eta] = \left(\frac{\eta_{rel} - 1}{c}\right)_{c=0} \tag{1}$$

as determined by extrapolation to $c = 0$[31] (e.g., see Figure S2 in the Supporting Information). The radius of hydration is estimated by

$$R_h = \left(\frac{3M[\eta]}{10\pi N_A}\right)^{\frac{1}{3}} \tag{2}$$

where M is the molecular weight of the polymer and N_A is Avogadro's number.[31−33]

Particle Synthesis. Monodisperse silica microspheres are synthesized with fluorescent cores composed of fluorescein isothiocyanate (FITC), following the procedure developed by van Blaaderen and co-workers.[34,35] Each microsphere consists of a 600 nm fluorescent silica core surrounded by a pure silica shell with an overall diameter of 1.02 ± 0.03 *μm*, as measured by scanning electron microscopy (Hitachi 4700, Tokyo, Japan). These fluorescent silica microspheres have a density of 2.0 g/cm³ and a specific surface area of 3.46 ± 0.04 m²/g, as determined by helium pycnometry and nitrogen gas adsorption, respectively.

Suspension Preparation. Colloidal suspensions of varying silica volume fraction (ϕ) are prepared by dispersing an appropriate amount of silica microspheres in an aqueous solution. Each suspension is magnetically stirred and ultrasonicated for 5 min using a 1 s on/off pulse sequence (F550 Sonic Dismembrator, Fisher Scientific). The pH is then adjusted using 0.1 and 1.0 M hydrochloric acid (HCl) or sodium hydroxide (NaOH) solutions. Next, an appropriate amount of either PTMAM-*g*-PEG or PTMAM is added to suspension from a 20 mg/mL stock solution, and the pH is readjusted. Each suspension is stirred for at least 10 min and then ultrasonicated, as described above, followed by stirring for an additional 12 h prior to settling under gravity. After sedimentation, the supernatant solution is decanted to remove excess (nonadsorbed) polymer. Finally, the silica microspheres are resuspended by adding an appropriate amount of a pH-adjusted aqueous solution to obtain the desired ϕ.

Polymer Adsorption Measurements. Colloidal silica suspensions ($\phi = 0.1$, pH 6.0) are prepared with varying concentrations of PTMAM-*g*-PEG or PTMAM ranging from 0 to 2.6 mg polymer/m² of silica in solution. After these suspensions undergo sedimentation, aliquots are taken from their supernatants and analyzed using ultraviolet−visible (UV−vis) spectroscopy (Shimadzu 2401PC, Kyoto, Japan) and total organic carbon (TOC) analysis (Phoenix 8000, Tekmar-Dohrmann, Mason, OH). The total amount of polymer adsorbed onto the silica microspheres is determined by subtracting the measured dispersant concentration in solution from the known initial concentration of PTMAM-*g*-PEG or PTMAM in solution.

Zeta Potential Measurements. The electrophoretic mobility of bare, PTMAM-*g*-PEG-coated, and PTMAM-coated silica microspheres is measured as a function of solution pH at a polymer concentration of 2.5 mg/m² of silica in solution. Colloidal silica suspensions ($\phi = 0.05$) are prepared with an initial pH of 6.0 and then adjusted to the desired pH of 3.0−8.5 using HCl or NaOH. The suspensions are then diluted ($\phi = 10^{-5}$) in water of the appropriate pH prior to measuring their electrophoretic mobility using a Malvern Zetasizer 3000 instrument (Worcestershire, U.K.). From these data, the zeta potential is determined using the Henry equation (see the Supporting Information).

Sedimentation Measurements. The sedimentation velocities of silica suspensions ($\phi = 0.02$, pH 6.0) are first measured as a function of dispersant concentration for both PTMAM-*g*-PEG and PTMAM in the absence of salt additions. Next, the sedimentation velocities of both systems ($\phi = 0.02$) prepared with a dispersant concentration of 2.5 mg/m² of silica in solution are measured as a function of varying salt concentration, [NaCl] = 0−1 M and pH. Specifically, each suspension is placed in a custom-designed cell and allowed to settle. The cells are created by attaching a glass cylinder (8 cm tall with a 5 mm inner diameter) to a no. 1 coverslip with silicon rubber. Images are acquired by a digital camera at regular intervals to monitor the interface between the clear supernatant and the opaque suspension. The measured sedimentation rate is normalized by U_o, which corresponds to that of an individual silica microsphere.[36]

(20) Lin, K. H.; Crocker, J. C.; Prasad, V.; Schofield, A.; Weitz, D. A.; Lubensky, T. C.; Yodh, A. G. *Phys. Rev. Lett.* **2000**, *85*, 1770–1773.

(21) Lin, S. Y.; Fleming, J. G.; Hetherington, D. L.; Smith, B. K.; Biswas, R.; Ho, K. M.; Sigalas, M. M.; Zubrzycki, W.; Kurtz, S. R.; Bur, J. *Nature (London)* **1998**, *394*, 251–253.

(22) Wong, S.; Kitaev, V.; Ozin, G. A. *J. Am. Chem. Soc.* **2003**, *125*, 15589–15598.

(23) Smay, J. E.; Gratson, G. M.; Shepherd, R. F.; Cesarano, J.; Lewis, J. A. *Adv. Mater.* **2002**, *14*, 1279.

(24) Caruso, F. *Adv. Mater.* **2001**, *13*, 11.

(25) Gref, R.; Minamitake, Y.; Peracchia, M. T.; Trubetskoy, V.; Torchilin, V.; Langer, R. *Science* **1994**, *263*, 1600–1603.

(26) Gupta, A. K. C.; Adam, S. G. *J. Mater. Sci.: Mater. Med.* **2004**, *15*, 493–496.

(27) LaVan, D. A.; McGuire, T.; Langer, R. *Nat. Biotechnol.* **2003**, *21*, 1184–1191.

(28) Hezinger, A. F. E.; Tessmar, J.; Gopferich, A. *Eur. J. Pharm. Biopharm.* **2008**, *68*, 138–152.

(29) Zhang, Y.; Kohler, N.; Zhang, M. Q. *Biomaterials* **2002**, *23*, 1553–1561.

(30) Mohraz, A.; Weeks, E. R.; Lewis, J. A. *Phys. Rev. E* **2008**, *77*, 4.

(31) Flory, P. J. *Principles of Polymer Chemistry*; Cornell University Press: Ithaca, NY, 1953.

(32) Taylor, T. J.; Stivala, S. S. *Polymer* **1996**, *37*, 715–719.

(33) Stevens, M. P. *Polymer Chemistry: An Introduction*, 3rd ed.; University of Hartford: 1999.

(34) van Blaaderen, A.; Vrij, A. *Langmuir* **1992**, *8*, 2921–2931.

(35) Verhaegh, N. A. M.; van Blaaderen, A. *Langmuir* **1994**, *10*, 1427–1438.

(36) Russel, W. B.; Saville, D. A.; Schowalter, W. R. *Colloidal Dispersions*; Cambridge University Press: New York, 1989.

$$U_o = \frac{2}{9} \frac{(\rho_s - \rho)a^2 g}{\eta} \qquad (3)$$

where ρ_s is the particle density, ρ is the density of water, a is the particle radius, η is the viscosity of water, and g is the gravitational constant.

Confocal Imaging. Colloidal suspensions of both PTMAM-g-PEG- and PTMAM-coated silica microspheres ($\phi = 0.02$) are prepared with a dispersant concentration of 2.5 mg/m² of silica in solution and varying salt concentration ($0 - 1$ M NaCl) and pH ($4.0 - 10.0$). Next, 0.5 mL of each suspension is immediately transferred to the custom-designed cells described above.[37] After undergoing sedimentation for 72 h, confocal microscopy is used to directly image their sediment structures by placing the samples on the stage of an inverted optical microscope equipped with a 514 nm argon-ion laser source and a 63/1.32 NA oil lens (Leica, SP2 Confocal Microscope, Wetzlar, Germany).

Results and Discussion

Polymer Synthesis and Characterization. The most attractive method for synthesizing the PTMAM-g-PEG comb polymer involves random copolymerization of a chain-end functionalized macromonomer with a low molecular weight monomer, as shown schematically in Figure 1a.[38] Using this method, the chain length of the polymer backbone can be controlled by living radical polymerization and the average spacing of the side chains can be determined by evaluation of the reactivity ratio of the low molecular weight monomer.[39] Initially, the copolymerization between DMAM and PEGMA was studied to determine whether the charge neutral teeth could be incorporated randomly along the polymer backbone. This involves determining the reactivity ratio (r_1) of the low molecular weight monomer, DMAM, from a Jaacks plot to determine $r_1(k_{11}/k_{12})$, which involves the use of a large excess of one monomer relative to another. This method allows for the assumption that all the propagating species in solution are derived from a single monomer, enabling the copolymer equation to be greatly simplified.[40]

To determine r_1 for DMAM [M_1] by the Jaacks method, the consumption of both monomers is monitored as a function of time in an uncontrolled free-radical copolymerization. A monomer feedstock of 20:1 DMAM:PEGMA is used to satisfy the assumption that all the propagating species in solution are derived from DMAM. Kinetic evaluation of the polymerization by GPC (Figure 1b) reveals a parallel decrease in the concentration of both monomers and concurrent increase in the concentration of comb polymer with time.[41] A plot of the conversion of each monomer with time indicates a slight preference for the consumption of DMAM relative to PEGMA with time, as shown in Figure 1c. A double logarithmic plot was constructed from which a linear relationship is observed between $\log([DMAM]_0/[DMAM]_t)$ and $\log([PEGMA]_0/[PEGMA]_t)$ (Figure 1c). The slope of the line gives a value of 1.24 for r_1, indicating a nearly random polymerization with a slight preference for consumption of DMAM by DMAM-derived chain ends.

To gain control over the polymerization, reversible addition−fragmentation chain transfer (RAFT) is employed. It was previously shown that selectivity of propagating radicals is
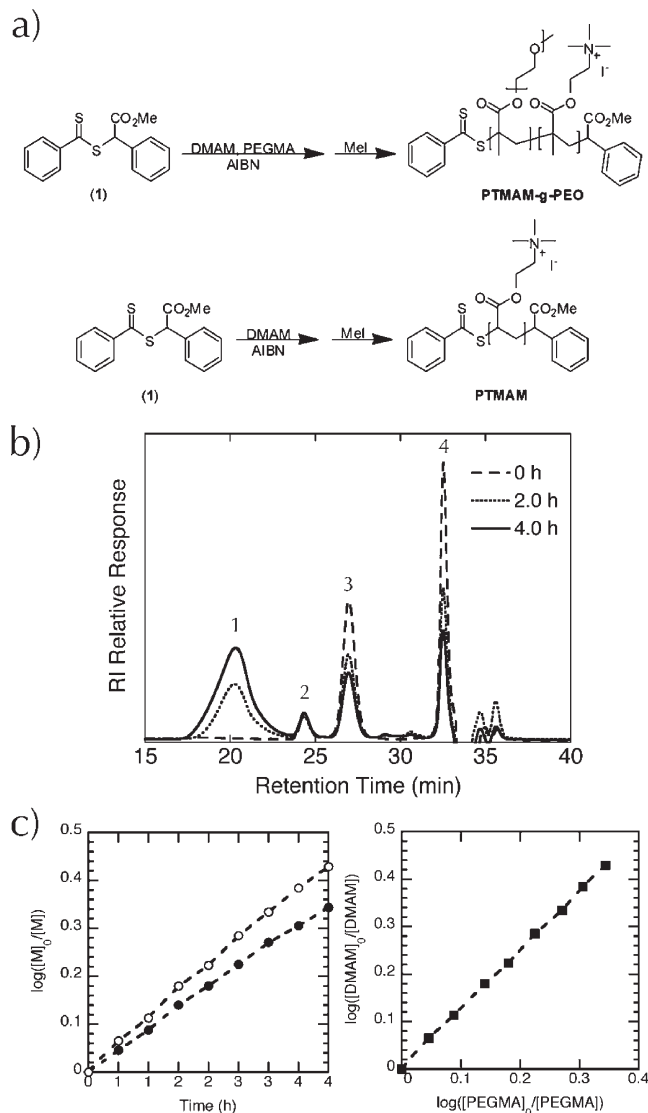
(37) Martinez, C. J.; Liu, J. W.; Rhodes, S. K.; Luijten, E.; Weeks, E. R.; Lewis, J. A. *Langmuir* **2005**, *21*, 9978–9989.
(38) Schulz, G. O.; Milkovich, R. J. *J. Appl. Polym. Sci.* **1982**, *27*, 4773–4786.
(39) Roos, S. G.; Muller, A. H.; Matyjaszewski, K. *Macromolecules* **1999**, *32*, 8331–8335.
(40) Jaacks, V. *Makromol. Chem.* **1972**, *161*, 161.
(41) Muehlebach, A. R., F. . *J. Polym. Sci., Part A: Polym. Chem.* 2003, 41, 3425.

a)

b)

c)

Figure 1. (a) Schematic of RAFT-mediated copolymerization of DMAM and PEGMA and homopolymerization of DMAM, (b) gel permeation chromatography of DMAM and PEGMA prior to reaction and after two and four hours of reaction, where peaks denoted by 1−4 correspond to the growing polymer, polystyrene standard, PEGMA, and DMAEMA, respectively, and (c) Jaacks plots of PEGMA (●) and DMAEMA (○) as a function of time (left) and a double logarithmic plot of $\log([DMAM]_0/[DMAM])$ and $\log([PEGMA]_0/[PEGMA])$ (right). [Note: Dashed lines guide the eye.]

independent of the polymerization mechanism, suggesting the reactivity ratio r_1 should hold true when going from an uncontrolled polymerization to a controlled polymerization by RAFT.[39] A large-scale polymerization was conducted, which yielded 134 g of the comb polymer and 48 g of homopolymer.

The pendant tertiary amine functionality along the polymer backbone is subsequently quaternized with excess methyl iodide (MeI) to form a strong cationic polyelectrolyte. This reaction is evaluated by ¹H NMR to confirm the quantitative conversion of tertiary amines to ammonium salts (see Figure S1 in the Supporting Information). DMAM is reacted with excess MeI to produce trimethylammonium iodide methacrylate (TMAM) to serve as a model compound for comparison. Prior to reaction with MeI, the methyl groups bound to the amine are observed at 2.18 ppm in both the DMAMA monomer and the copolymer. After reaction

with MeI, the signal at 2.18 ppm is absent in both the model compound and the copolymer, indicating quantitative conversion. Interestingly, the resonance assigned to the ammonium methyl groups is shifted downfield in the polymer relative to the model compound.

Polymer Solution Behavior. The PTMAM-based dispersants are fully charged from pH 3 to 9 based on titration data (not shown). We find that the radius of hydration, R_h, of PTMAM-*g*-PEG and PTMAM is approximately 12 and 8.3 nm, respectively, at the lowest salt concentration of 1 mM evaluated (Figure 2). Under these conditions, the charged polymer chains are expected to adopt an extended conformation in solution. When the salt concentration is increased to 10 mM, the R_h of both species decreases sharply to values of 10.4 and 6.6 nm, respectively, as the charge groups along their cationic backbones are increasingly screened. At even higher salt concentrations, the PTMAM-*g*-PEG and PTMAM chains undergo further collapse to final sizes of 9.0 and 4.7 nm, respectively, at 1 M salt. When the R_h of PTMAM-*g*-PEG and PTMAM is normalized by their
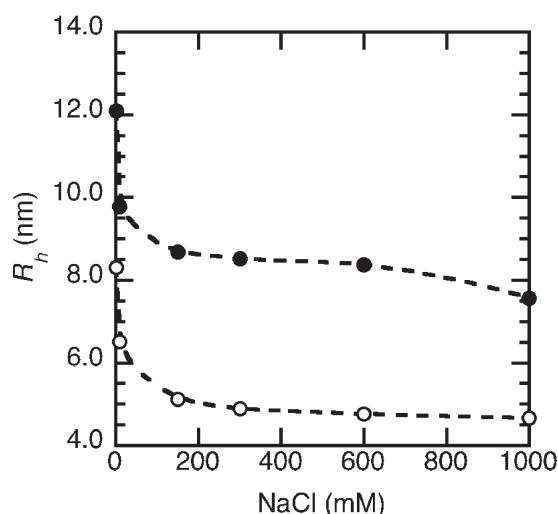

Figure 2. Plot of the radius of hydration (R_h) of PTMAM-*g*-PEG (●) and PTMAM (○) in dilute solution (2 wt %, pH 6.0) as a function of salt concentration. [Note: Dashed lines guide the eye.]
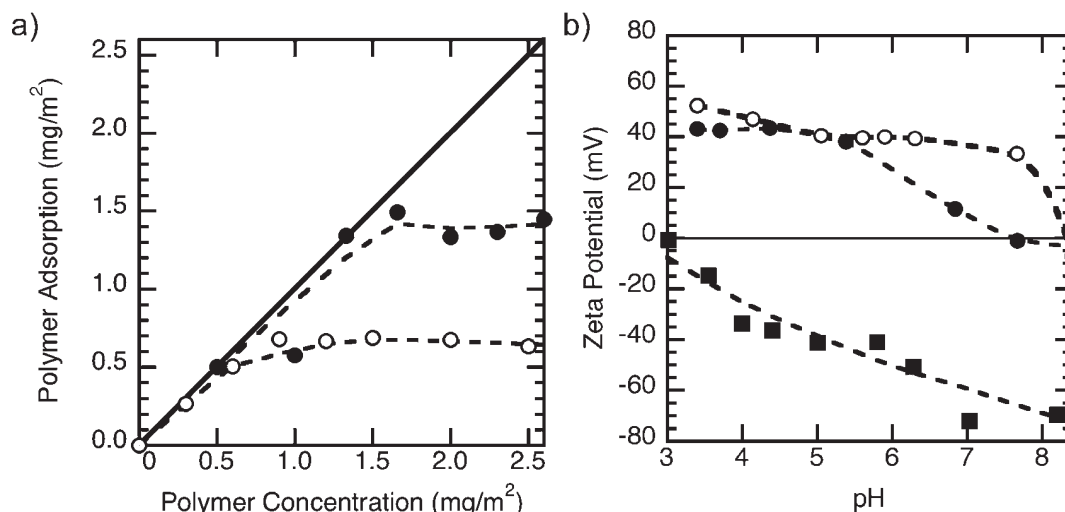
respective values at 1 mM salt, one finds that their size is reduced approximately 30% and 40%, respectively, at the highest salt concentrations probed. Both polymers undergo a similar size reduction, which suggests that the relatively short PEG teeth do not significantly hinder the conformational changes of the PTMAM backbone induced at high ionic strengths.

Polymer Adsorption Behavior. Both PTMAM-*g*-PEG and PTMAM strongly adsorb onto oppositely charged silica microspheres leading to their pronounced charge reversal, as shown in Figure 3. As the polymer concentration in solution increases, there is a sharp rise in the extent of adsorption of both polymers followed by the onset of a plateau at values of 1.41 and 0.66 mg/m² for PTMAM-*g*-PEG and PTMAM, respectively (Figure 3a). Note, the polymer concentrations reported in Figures 3a and 4a relate the polymer mass to the total colloid surface area in solution, thereby allowing direct comparison to be made between experiments carried out at different ϕ. The marked difference in plateau coverage for these polymers is attributed primarily to the presence or absence of PEG teeth, since the actual number of cationic groups in each adlayer is nearly identical, that is, 2.5×10^{18} and $2.3 \times 10^{18}/m^2$ for PTMAM-*g*-PEG and PTMAM, respectively.

In the absence of either dispersant, the bare silica microspheres possess an isoelectric point at approximately pH 3. The microspheres become more negatively charged as the pH is raised above this value (see Figure 3b). Under the experimental conditions of interest (pH 6), the silica microspheres exhibit a zeta potential of −50 mV. Upon suspending the silica microspheres in polymer solutions composed of 2.5 mg/m², they become fully coated with either PTMAM-*g*-PEG or PTMAM. The presence of the cationic adlayer increases the zeta potential of the coated silica microspheres by ca. 60−80 mV over the entire pH range explored, shifting their isoelectric point to a value near pH 8. Hence, the PTMAM-*g*-PEG and PTMAM-coated silica microspheres are positively charged at a pH of 6 with respective zeta potentials of 20−40 mV.

Colloidal Suspension Stability. The stability of silica microspheres as a function of dispersant concentration is investigated by measuring the sedimentation rates of dilute suspensions ($\phi = 0.02$) (Figure 4a). Bare silica microspheres are stable at pH 6 and, thus, settle individually ($U/U_o \sim 1$). When the
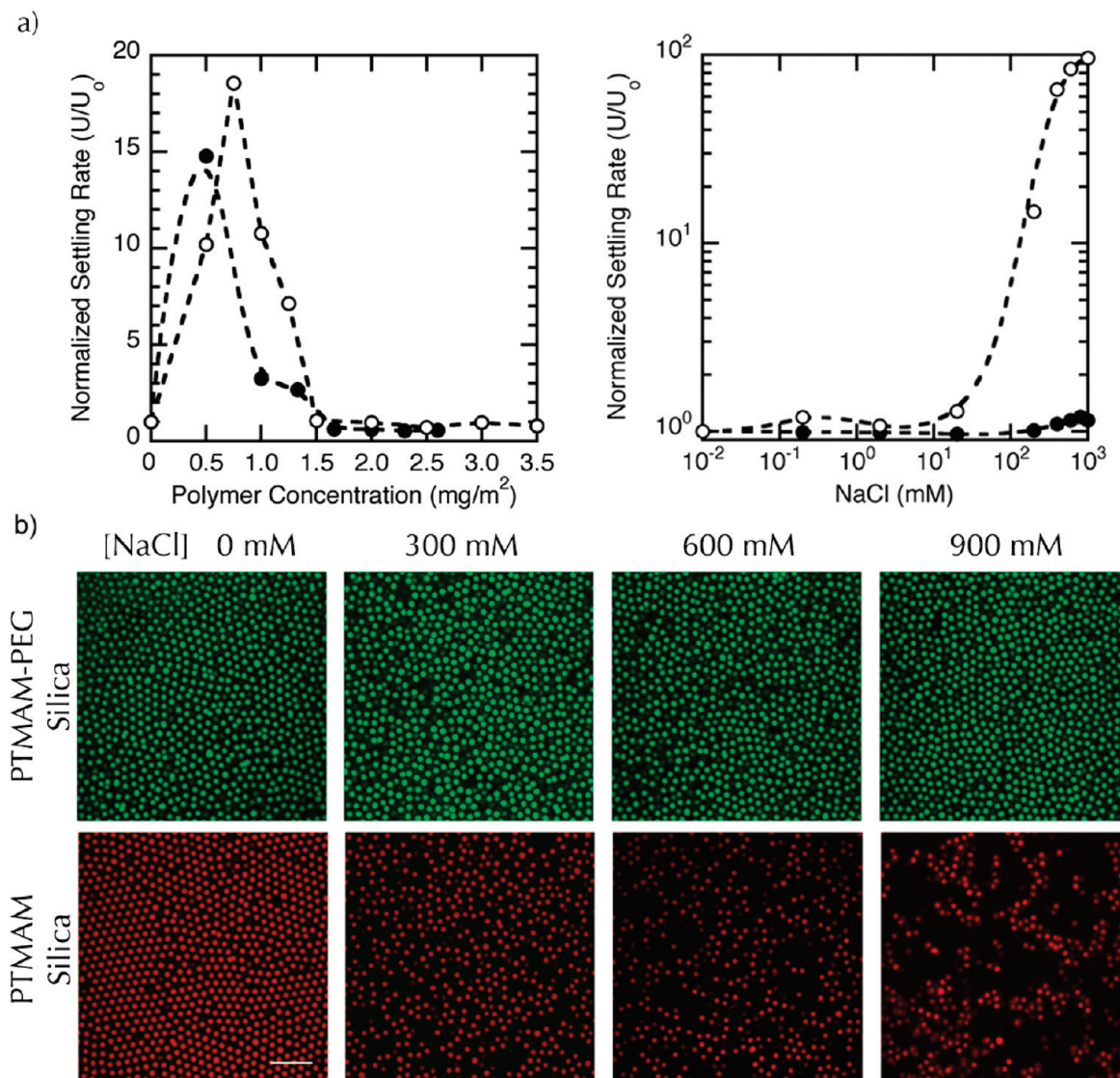

Figure 3. (a) Adsorption behavior of PTMAM-*g*-PEG (●) and PTMAM (○) on oppositely charged silica microspheres in aqueous suspensions ($\phi = 0.1$, pH 6) of varying dispersant concentration, where the solid line denotes the theoretical curve corresponding to 100% adsorption, and (b) zeta potential of bare (■), PTMAM-*g*-PEG-coated (●), and PTMAM (○)-coated silica microspheres as a function of pH for dilute aqueous suspensions ($\phi = 10^{-5}$) with a polymer concentration of 2.5 mg/m² of silica in solution. [Note: Dashed lines guide the eye.]

Figure 4. (a) Normalized settling rate of PTMAM-*g*-PEG-coated (●) and PTMAM (○)-coated silica microspheres in aqueous suspensions ($\phi = 0.02$, pH = 6.0) as a function of polymer concentration at 0 mM salt (left plot) or as a function of increasing salt concentration at a normalized polymer concentration of 2.5 mg/m² of silica in solution (right plot), and (b) confocal images (*x*−*y* scans) of representative sediment structures assembled from the latter suspensions. [Note: Dashed lines guide the eye; scale bar = 5 μm for all images.]

oppositely charged PTMAM-*g*-PEG and PTMAM species adsorb onto the silica microspheres at modest concentrations, they diminish the electrostatic repulsion between particles, leading to a pronounced rise in the observed sedimentation rates. The highest sedimentation rates, which occur at normalized polymer concentrations in solution of 0.4−0.7 mg/m², are roughly 15−20 times greater than those of individual silica microspheres. As the polymer concentration is further increased, the sedimentation rates decrease. Ultimately, when the normalized polymer concentration exceeds approximately 1.5 mg/m², the silica microspheres settle individually, signifying that full stabilization has been achieved.

The effect of ionic strength on the stability of PTMAM-*g*-PEG-coated and PTMAM-coated silica suspensions is studied to probe the role of dispersant architecture. In the absence of salt additions, each system is stable and the dispersant-coated silica microspheres settle individually. Hence, at low ionic strength, both dispersants impart electrosteric stability to the silica microsphere suspensions. At higher ionic strengths, the charged backbone of each dispersant becomes increasingly screened, and only PTMAM-*g*-PEG remains able to confer

suspension stability. In fact, silica microspheres coated with PTMAM-*g*-PEG exhibit low sedimentation rates, which are nominally equivalent to those observed for individual microspheres, over the entire range of salt concentrations studied (0−1 M salt), as shown in Figure 4a. We attribute the observed stabilization to the presence of the charge-neutral PEG teeth along the PTMAM backbone, which continue to provide a steric barrier even as the electrostatic contribution is diminished. By contrast, PTMAM-coated silica microspheres exhibit a pronounced rise in their sedimentation rates when the salt concentration exceeds ~30 mM.

To further probe the influence of dispersant architecture on suspension stability, confocal microscopy is used to directly image the sediment structures formed in each system as a function of salt concentration. In the absence of added salt, both PTMAM-*g*-PEG-coated (green microspheres) and PTMAM-coated (red microspheres) colloids are stable and assemble into dense, ordered structures upon sedimentation, as shown in Figure 4b. This morphology persists, even at the highest ionic strengths investigated for silica microspheres coated with PTMAM-*g*-PEG species. By contrast, PTMAM-coated silica microspheres
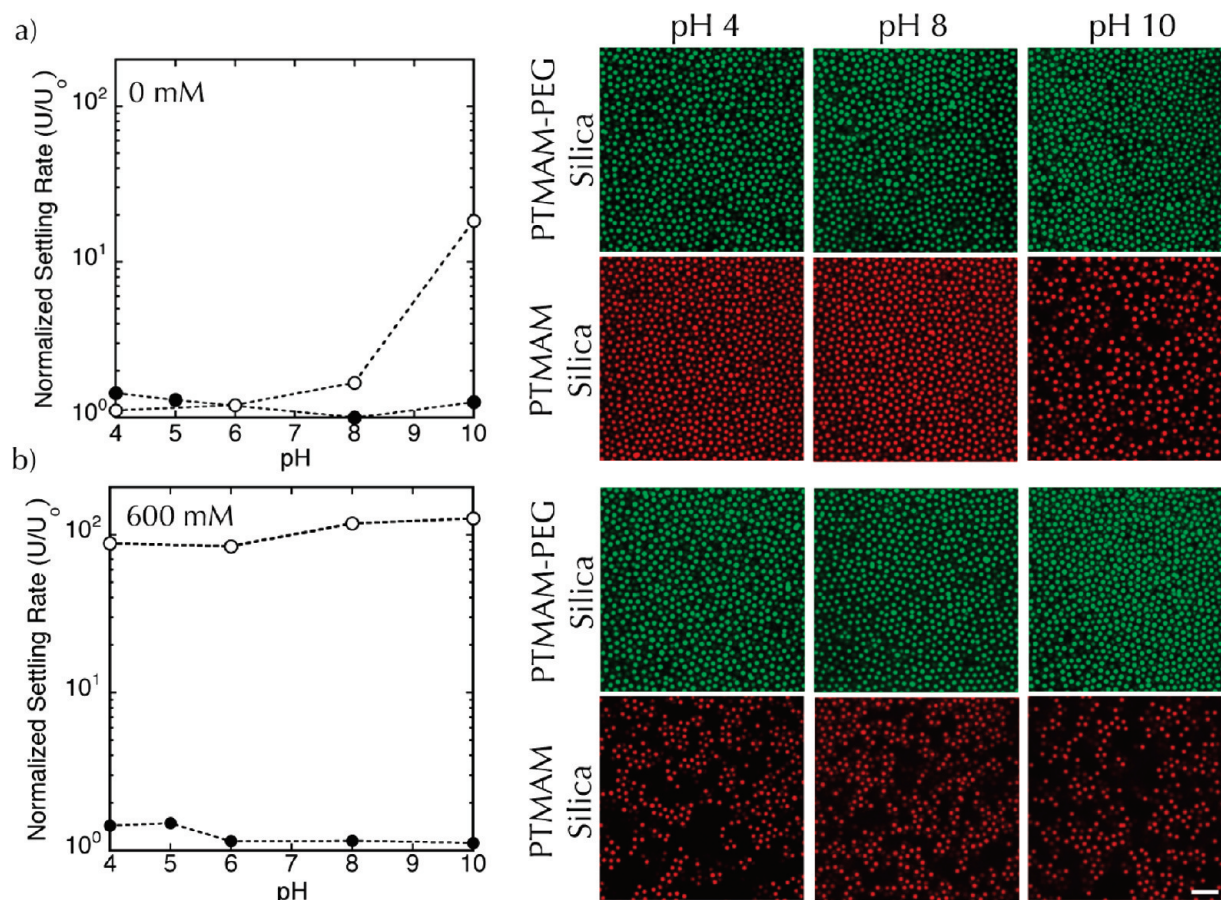
Figure 5. Normalized settling rates of PTMAM-*g*-PEG-coated (●) and PTMAM (○)-coated silica microspheres in aqueous suspensions (ϕ = 0.02, polymer concentration of 2.5 mg/m^2 of silica in solution) as a function of pH and accompanying confocal images (*x*−*y* scans) of representative sediment structures assembled at pH 4, 8, and 10 for systems prepared at (a) 0 mM and (b) 600 mM NaCl. [Note: Dashed lines guide the eye; scale bar = 5 μm for all images; and images obtained at pH 6 are shown in Figure 4.]

undergo flocculation at high ionic strengths, resulting in an open, gel network that consists of dense clusters and large voids. The structural evolution observed for each system as a function of ionic strength is consistent with their sedimentation behavior, as described above.

We studied the stability of PTMAM-*g*-PEG and PTMAM-coated silica suspensions under varying pH conditions to further evaluate dispersant effectiveness. In the absence of salt additions, both systems are stable over a pH range from 4 to 8, as shown in Figure 5a. At pH 10, only silica microspheres coated with PTMAM-*g*-PEG remain stable and exhibit $U/U_o \sim 1$. By contrast, PTMAM-coated silica microspheres rapidly flocculate at pH 10, leading to an order of magnitude higher sedimentation rate. Representative confocal images obtained on their sediment structures reveal that all samples assemble into dense, ordered structures at low ionic strengths over the entire pH range probed, with the exception of the PTMAM-coated silica microspheres at pH 10, which forms an open, gel network that consists of dense clusters and large voids.

Finally, we investigated the stability of PTMAM-*g*-PEG-coated and PTMAM-coated silica suspensions under varying pH conditions at high ionic strengths (i.e., 600 mM salt). Over the full range of solution conditions tested, PTMAM-*g*-PEG-coated silica microspheres remained stable and settled individually under gravity to produce dense, ordered structures, whereas the PTMAM-coated silica microspheres exhibited pronounced flocculation, leading to an open gel-like structure and sedimentation rates that are two orders of magnitude higher than those of

their stable counterparts (Figure 5b). Our observations confirm that comb polymers are effective "superdispersants" that impart stability over a broad range of solution conditions, where pure polyelectrolyte species fail.

Conclusions

We have shown that dispersant architecture dramatically influences the ability of cationic polyelectrolytes to impart stability to silica suspensions of varying ionic strength and pH. Dispersants that possess a comb polymer architecture composed of a cationic backbone and charge-neutral teeth are able to bestow stability to colloidal silica suspensions over a broad range of solution conditions. These "superdispersants" may find potential application in suspensions designed for colloidal crystallization, biphasic inks for direct-write assembly, drug delivery, or other biomedical applications.

Supporting Information Available: Details of the polymer synthesis and characterization are provided. The calculations used to determine the reported zeta potential measurements from the measured electrophoretic mobilities are also described. This material is available free of charge via the Internet at http://pubs.acs.org.